The CRISPR Journal

RESEARCH ARTICLE

Functional Characterization of Type III-A CRISPR-Cas in a Clinical Human Methicillin-R *Staphylococcus aureus* Strain

Yang Li,[1,2] Kasper Mikkelsen,[3] Oleguer Lluch i Grané,[3] Zhenyu Wang,[1,2] Yuanyue Tang,[1,2,4] Xinan Jiao,[1,2,4] Hanne Ingmer,[3] Nina Molin Høyland-Kroghsbo,[5,*] and Qiuchun Li[1,2,4,*]

Abstract

CRISPR with its *cas* genes is an adaptive immune system that protects prokaryotes against foreign genetic elements. The type III-A CRISPR-Cas system is rarely found in *Staphylococcus aureus*, and little is known about its function in *S. aureus*. Here, we describe the genome characteristics of the clinical methicillin-resistant *S. aureus* (MRSA) strain TZ0912, carrying a type III-A CRISPR-Cas system. Phylogenetic analysis of 35 reported CRISPR-Cas-positive *S. aureus* strains revealed that the CRISPR-Cas system is prevalent in CC8 clones (10/35) and is located in the staphylococcal cassette chromosome *mec* (SCC*mec*) V, which confers methicillin resistance. Plasmid transformation and phage infection assays reveal that the type III-A CRISPR-Cas system protects TZ0912 against foreign DNA with sequence homology to the spacers located in the CRISPR array. We observed that the CRISPR-Cas immune system could effectively protect MRSA against phage attacks in both liquid culture and solid medium. In accordance with previous reports, using RNA-seq analysis and plasmid transformation assays, we find that the crRNAs close to the leading sequence of the CRISPR array are more highly expressed and are more effective at directing plasmid elimination compared to the distant spacers. This study established a model for evaluating the efficiency of naive CRISPR-Cas system in MRSA against phage, which could contribute to future research on the function of CRISPR-Cas in clinical MRSA isolates and improve phage therapy against MRSA infections.

Introduction

CRISPR-Cas is an adaptive immune system that protects bacteria and archaea against invasion of foreign genetic elements.[1,2] Approximately 40% of genome sequenced bacteria and 81% of archaea harbor CRISPR-Cas systems.[3] Based on the composition of *cas* genes, CRISPR-Cas systems are classified into two classes, six types (I–VI) with 33 subtypes.[4] The type III system can target both DNA and RNA and is considered to be the most ancient type of the CRISPR-Cas systems.[5] Currently, the type III system can be divided into six subtypes: III-A, III-B, III-C, III-D, III-E, and III-F.[4] The immunity process mediated by the type III-A CRISPR-Cas occurs in three stages termed "adaptation," "CRISPR RNA

(crRNA) biogenesis," and "interference." During adaption, short nucleic acid sequences from invading genetic elements are integrated into the CRISPR arrays as spacers by the Cas1–Cas2 complexes to provide a "memory" of the invasion.[6–9] The CRISPR arrays are transcribed and processed into mature crRNAs by Cas6 protein and host nucleases.[10–12] The mature crRNAs can guide the type III-A effector complex to recognize complementary RNA targets, which activates cleavage of nonspecific ssDNA by Cas10.[13,14] In addition, the target RNA binding by the effector complex triggers Cas10 Palm domains to synthesize the second messenger cyclic oligoadenylates (cOAs), which then activates the Csm6 RNase by binding to its CRISPR-associated Rossmann fold

[1]*Jiangsu Key Lab of Zoonosis/Jiangsu Co-Innovation Center for Prevention and Control of Important Animal Infectious Diseases and Zoonoses, Yangzhou University, P.R. China;* [2]*Key Laboratory of Prevention and Control of Biological Hazard Factors (Animal Origin) for Agri-food Safety and Quality, Ministry of Agriculture of China, Yangzhou University, P.R. China;* [3]*Department of Veterinary and Animal Sciences, University of Copenhagen, Copenhagen, Denmark;* [4]*Joint International Research Laboratory of Agriculture and Agri-Product Safety, Yangzhou University, P.R. China;* and [5]*Department of Plant and Environmental Sciences, University of Copenhagen, Copenhagen, Denmark.*

Address correspondence to: Nina Molin Høyland-Kroghsbo, PhD, Department of Plant and Environmental Sciences, University of Copenhagen, Copenhagen, Denmark, Email: nmhk@plen.ku.dk*; and Qiuchun Li, PhD, Jiangsu Key Lab of Zoonosis/Jiangsu Co-Innovation Center for Prevention and Control of Important Animal Infectious Diseases and Zoonoses, Yangzhou University, P.R. China,* Email: qcli@yzu.edu.cn

(CARF) domain.[15,16] The activated Csm6 can nonspecifically degrade both the targeted and host RNA transcripts.[17,18] The efficacy of the CRISPR-Cas systems in protecting bacteria from foreign invading elements is highly variable and depends on a range of factors, including environmental factors and protein inhibitors encoded on, for example, phages.[19–24]

The type III-A CRISPR-Cas system is not prevalent in *Staphylococcus aureus*, with only 0.94% (6/636) of clinical strains reported to harbor the system.[25] *S. aureus* is an opportunistic pathogen that naturally colonizes humans and animals, but it also gives rise to a wide range of infections. Particularly concerning are infections with methicillin-resistant *S. aureus* (MRSA), where resistance is provided by the *mecA* gene located within the staphylococcal chromosomal cassette element, SCC*mec*.[26] In the *S. aureus* strain 08BA02176 and *Staphylococcus argenteus* MSHR1132, the CRISPR-*cas* locus is located in the SCC*mec*, suggesting that the system may be mobile.[27] The majority of CRISPR-Cas systems in *Staphylococci* belong to the type III-A system and are localized in the SCC*mec* (Table 1).[25,28–30] It has been reported that the type III-A CRISPR-Cas system in clinical *S. aureus* isolates provides resistance against plasmid invasion.[25] Type III-A CRISPR-Cas systems are also found in the related species *Staphylococcus epidermidis* at a frequency of 14%[31] where it provides resistance to both plasmid invasion and phage infection.[2,17,18]

Here, we characterize the type III-A CRISPR-Cas system located in the human clinical MRSA strain TZ0912 originating from China. Comparative genomic analysis show that the majority of type III-A CRISPR-Cas-positive *S. aureus* belong to CC8 clones, which are clustered separately in the phylogenetic tree. The CRISPR-Cas system can protect the bacteria from plasmids and the virulent philPLA-RODI phage carrying protospacers targeted by the CRISPR-Cas system. During phage infection, cells grown in liquid culture show stronger CRISPR-Cas immunity against phage than those cultured on solid media. Further, we demonstrate that crRNAs in proximity to the leader region in the CRISPR array are more highly expressed and result in the stronger immunity compared to crRNAs expressed from more distant spacers.

Methods

Bacterial strains, plasmids, and growth conditions
The bacterial strains, phage, and plasmids used in this study are listed in Supplementary Table S1. The MRSA RN4220 or TZ0912 and *Escherichia coli* IM08B were grown in tryptic soy broth (TSB) and LB Broth (Lennox) media, respectively, at 37°C. The media were supplemented with ampicillin 100 μg/mL or chloramphenicol 25 μg/mL for *E. coli* and chloramphenicol 15 μg/mL for *S. aureus* to ensure plasmid maintenance.

Whole-genome sequencing, molecular typing, and bioinformatics analysis
Whole-genome sequencing was carried out on the PacBio Sequel platform and Illumina NovaSeq PE150 (Illumina). The CRISPR-Cas system in TZ0912 was identified using CRISPRCasFinder.[32] The CRISPRTarget tool was used to find the sequences homologous to spacers in the NCBI database.[33] The molecular typing, including multi-locus sequence typing (MLST), *spa* typing, and SCC*mec* typing, were performed in the typing webserver (https://cge.cbs.dtu.dk/services/). Maximum-likelihood phylogenetic reconstruction of the 35 CRISPR-Cas-positive *S. aureus* isolates for the core genome regions was performed by Parsnp software.[34] The antimicrobial susceptibility testing of TZ0912 was conducted using the disk-diffusion method in Mueller-Hinton agar (BD Difco™) following the standards enacted by the Clinical and Laboratory Standards Institute in 2018.

Construction of plasmids and mutants
For construction of the CRISPR-targeted plasmid, the protospacer sequence was annealed and then cloned into the pRAB11 plasmid[35] between restriction cites *EcoR*I and *Bgl*II to get pCR1SP1, pCR1SP6, and pCR1SP14 plasmids with three sets of primers: PT1/PT2, PT3/PT4, and PT5/PT6, respectively.[36] The primers

Table 1. Previously Reported CRISPR-Cas Systems Identified in *Staphylococcus aureus*

Strain	CRISPR-Cas type	CRISPR-Cas activity	SCCmec type	Located in SCCmec	ST type	Location	Reference
08BA02176	III-A	Not confirmed	V	Yes	ST398	Saskatchewan, Canada	[28]
AH1	III-A	Functional	V	Yes	10-n-8-6-10-3-2	Anhui, P.R. China	[25]
AH2	III-A	Not confirmed	V	Yes	ST630	Anhui, P.R. China	[25]
AH3	III-A	Not confirmed	V	Yes	ST630	Anhui, P.R. China	[25]
SH1	III-A	Not confirmed	V	Yes	ST630	Shanghai, P.R. China	[25]
SH2	III-A	Not confirmed	V	Yes	ST630	Shanghai, P.R. China	[25]
JS395	III-A	Not confirmed	V	Yes	ST1093	Geneva, Switzerland	[30]
M06/0171	II-C	Not confirmed	Novel type	Yes	ST779	Dublin, Ireland	[29]

and protospacers used in this study are listed in Supplementary Table S2. The sequences of pCR1SP1, pCR1SP6, and pCR1SP14 plasmids are shown in the Supplementary Sequence Data. The construction of the TZ0912 ΔCRISPR Δcas mutant was carried out using the homologous recombination method, as described previously.[37] In brief, DNA fragments flanking the CRISPR-Cas locus were amplified using the primers P1/P2 and P3/P4. The two polymerase chain reaction (PCR) products were then cloned into pIMAY plasmid using NEBuilder HiFi DNA Assembly Master Mix. The resulting plasmids were transformed into *E. coli* DC10B, purified, and transformed into *S. aureus* TZ0912 followed by plating onto tryptic soy agar (TSA) containing 15 μg/mL chloramphenicol at 28°C for 16 h. To integrate the recombinant plasmid into the chromosome, the transformants were streaked onto TSA containing 15 μg/mL chloramphenicol and incubated at 37°C. Colonies undergoing upstream or downstream crossover were inoculated into TSB without chloramphenicol at 28°C overnight to stimulate rolling circle replication. The overnight cultures were then plated onto TSA containing 1 μg/mL anhydrotetracycline (ATc) at 28°C for 24 h, which aimed to remove the plasmid in the cells. Colonies were patched on TSA containing ATc and TSA containing 15 μg/mL chloramphenicol, respectively, and grown at 37°C overnight. Putative mutants (chloramphenicol-sensitive colonies) were confirmed by PCR and sequencing using the primer P5/P6.

Preparation of electrocompetent *S. aureus* cells

Overnight cultures of *S. aureus* TZ0912 or RN4220 were grown in 10 mL TSB in 50 mL flasks and diluted to an optical density at 600 nm (OD_{600}) of 0.5 in fresh TSB media. The cultures were re-incubated at 37°C for 40 min and then cooled on ice for 10 min, with all subsequent steps performed at 4°C or on ice. The cells were collected at 4,000 g for 10 min, and two washes were performed with equal volume of ice-cold sterile water. The cells were then repeatedly centrifuged and re-suspended first in 1/5, then in 1/10, and ultimately in 1/200 the volume of ice-cold sterile 10% glycerol. Aliquots (50 μL) were frozen at −70°C.

Transformation efficiency assay

The plasmid DNA was extracted by using the GeneJET Plasmid Midiprep Kit (Thermo Fisher Scientific) according to the manufacturer's instructions and then quantified using a NanoDrop 2000c Spectrophotometer (Thermo Fisher Scientific). For electroporation, 5 μg plasmid DNA was electroporated into 50 μL competent cells using a MicroPulser electroporator (Bio Rad) with the following parameters: 2.1 kV, 25 μF, 100 Ω.[37] TSB (1 mL) supplemented with 500 mM sucrose was added immediately after electroporation, and the transformants were grown at 37°C shaking at 180 rpm for 1 h. All of the cells were plated on the TSA plates containing 15 μg/mL chloramphenicol and 150 ng/mL ATc and incubated at 37°C for 24 h before enumerating colony-forming units (CFU). The efficiency of transformation (EOT) was calculated, as described previously.[21] Briefly, the CFU/mL were quantified, and the EOT was calculated as the percentage colonies transformed by pCR1SP1, pCR1SP6, and pCR1SP14 compared to those transformed by the pRAB11 plasmid.

Growth curve

Overnight cultures of *S. aureus* were diluted to an OD_{600} of 0.05 in 30 mL TSB with 5 mM $CaCl_2$ and incubated at 37°C with shaking for 1 h. The phage was then added at a multiplicity of infection (MOI) of 5. The OD_{600} was measured every hour. Experiments were repeated three times.

Plaque assay

Overnight cultures of the wild-type TZ0912 and the TZ0912 ΔCRISPR Δcas mutant were mixed with soft TSB agar and then dispersed evenly on TSA. A series of 10-fold dilutions of the phiIPLA-RODI phage were spotted on the lawns of TZ0912 and TZ0912 ΔCRISPR Δcas mutant. The plates were incubated at 37°C and imaged the next day. To count the plaques, full plate assays were used. For full plate assays, 25 μl phage dilution (about 250 PFU) was incubated with 50 μL *S. aureus* overnight culture for 10 min at 37°C. Soft TSB agar (5 mL) was then added, and the mixture was poured onto a TSA. Individual plaques were then counted, and the efficiency of plaquing (EOP) was calculated.

Loss of plasmid assay

Single fresh *S. aureus* colonies of each transformation experiment with pCR1SP1 plasmid were picked and re-suspended in 50 μL TSB. Triplicates of 5 μL were inoculated in 5 mL TSB 0.6 μM ATc and then were incubated at 37°C for 20 h. After the incubation time, cultures were serially diluted and plated on TSB agar and TSB agar with 15 μg/mL chloramphenicol and incubated overnight at 37°C before enumerating the CFUs.

Quantitative reverse transcription PCR

The *S. aureus* TZ0912 cells were harvested after 20 h of growth in liquid or solid culture. RNA was extracted from cells treated with 5 μL lysostaphin (5 mg/mL) at 37°C for 1 h in 180 μL lysozyme buffer using a RNeasy Mini Kit following the manufacturer's protocol (Qiagen). The removal of gDNA and reverse transcription (RT) reactions

were performed using PrimeScript RT regent kit with gDNA Eraser (Takara), after which quantitative RT-PCR (qRT-PCR) was carried out using FastStart Universal SYBR Green Master (ROX; Roche).

RNA-seq

Overnight cultures were diluted to an OD_{600} of 0.05 in 30 mL TSB and then incubated at 37°C with shaking for 9 h. The cells were harvested at the indicated time points. RNA was extracted from cells treated with 5 μL lysostaphin (5 mg/mL) at 37°C for 1 h in 180 μL lysozyme buffer using a RNeasy mini kit following the manufacturer's protocol (Qiagen). RNA libraries were prepared with a TruSeq RNA Sample Prep Kit (Illumina) and then were sequenced on an Illumina HiSeq2000 sequencer. The RNA-seq reads were trimmed and mapped to TZ0912 genome. The locations of these mapped reads were summarized as a coverage plot by using Integrative Genomics Viewer.[38]

Results

General characterization of the type III-A CRISPR-Cas system in *S. aureus* TZ0912

The MRSA strain TZ0912 was isolated from a patient with a skin infection in the Taizhou Hospital in China. The genome of MRSA *S. aureus* TZ0912 is composed of a unique circular chromosome of 2.91 Mb (SRA accession: ERS5337611; Supplementary Fig. S1). The whole genome sequence revealed that TZ0912 harbors a CRISPR-Cas system located in a SCC*mec* type V resistance cassette (Fig. 1A). In addition, we also found that the TZ0912 strain is sequence type 630 (ST630) and *spa* type t4549, and it is resistant to cefoxitin, erythromycin, and penicillin.

CRISPRCasFinder analysis showed that TZ0912 carries a classical type III-A CRISPR-Cas system with nine *cas-csm* genes flanked by two CRISPR arrays (Fig. 1B). The CRISPR1 array of stain TZ0912 has 15 spacers, while the CRISPR2 has two spacers (Fig. 1C). To identify putative targets of the TZ0912 CRISPR-Cas system, we examined whether the CRISPR spacers show homology to plasmid or phage sequences in the NCBI database. Of the 17 total CRISPR spacers in TZ0912, 11 are predicted to target known sequences from phages or plasmids (Table 2). Among these, spacer 6 displays 97% identity (one mismatch) to the long terminal repeats (*ltr*) region of the lytic *Staphylococcus* phage philPLA-RODI (Fig. 1D). Spacer 10 shows 80% identity to phage 6ec, and this spacer is prevalent in many CRISPR arrays found in *S. epidermidis* strains.[31]

The type III-A CRISPR-Cas system is prevalent in *S. aureus* CC8 clones

To characterize further the *S. aureus* strains that harbor CRISPR-Cas, we analyzed all available 12,582 whole genome sequences of *S. aureus* from the NCBI database using CRISPRCasFinder.[32] A total of 35 *S. aureus* genomes, including MRSA TZ0912, were found to encode complete type III-A CRISPR-Cas systems (Supplementary Table S3), with the predominant sequence types ST630 (7/35), ST45 (7/35), and ST398 (6/35). Interestingly, for 30 out of these 35 genomes, the CRISPR-Cas system was located within the SCCmec type V resistance cassette, indicating that the CRISPR-Cas system could be mobile. Among the 35 CRISPR-Cas-positive *S. aureus*, 27 *S. aureus* isolates were isolated from humans, while only two and one isolates were isolated from animals

FIG. 1. The CRISPR-*cas* system in methicillin-resistant *Staphylococcus aureus* (MRSA) TZ0912. **(A)** Schematic diagram showing the chromosomal location of the CRISPR-*cas* system in MRSA TZ0912. The CRISPR-*cas* system is located in the staphylococcal cassette chromosome *mec* (SCC*mec*) V element. *Different-colored arrows* indicate the direction of transcription of the different genes. The boundaries direct repeats (DR) of SCC element are represented by vertical lines. DR_L: AGAAGCGTATCACAAATAA, DR_R: AGAAGCATATCATAAATGA. **(B)** The type III-A CRISPR-*cas* locus (10,012 bp) in TZ0912 contains nine *cas* genes with two CRISPR arrays. The *cas* genes within the same functional groups are presented in the same color. The CRISPR 1 and CRISPR 2 arrays (in *red*) encode the crRNAs. The *cas1* and *cas2* genes (in *green*) encode the Cas proteins responsible for integrating the new spacers into the CRISPR arrays. The Type III-A effector complex composed of the proteins encoded by *cas10*, *cas11*, *cas7*, *cas5*, and *cas7* (in *blue*) bind a crRNA and target foreign nucleic acids. The *csm6* (in *yellow*) encodes a nonspecific RNase, and *cas6* (in *pink*) is involved in the process of pre-crRNA processing. **(C)** The CRISPR 1 and CRISPR 2 arrays contain 15 and 2 spacers, respectively (unique spacers are colored and numbered). The *black diamonds* represent repeats. The *arrow* indicates the predicted direction of transcription. **(D)** Alignment of CRISPR 1 spacer 6 (CR1SP6) from TZ0912 with the protospacer in philPLA-RODI. There is one mismatch between the CR1SP6 crRNA and the protospacer *ltr* target (highlighted in *red*).
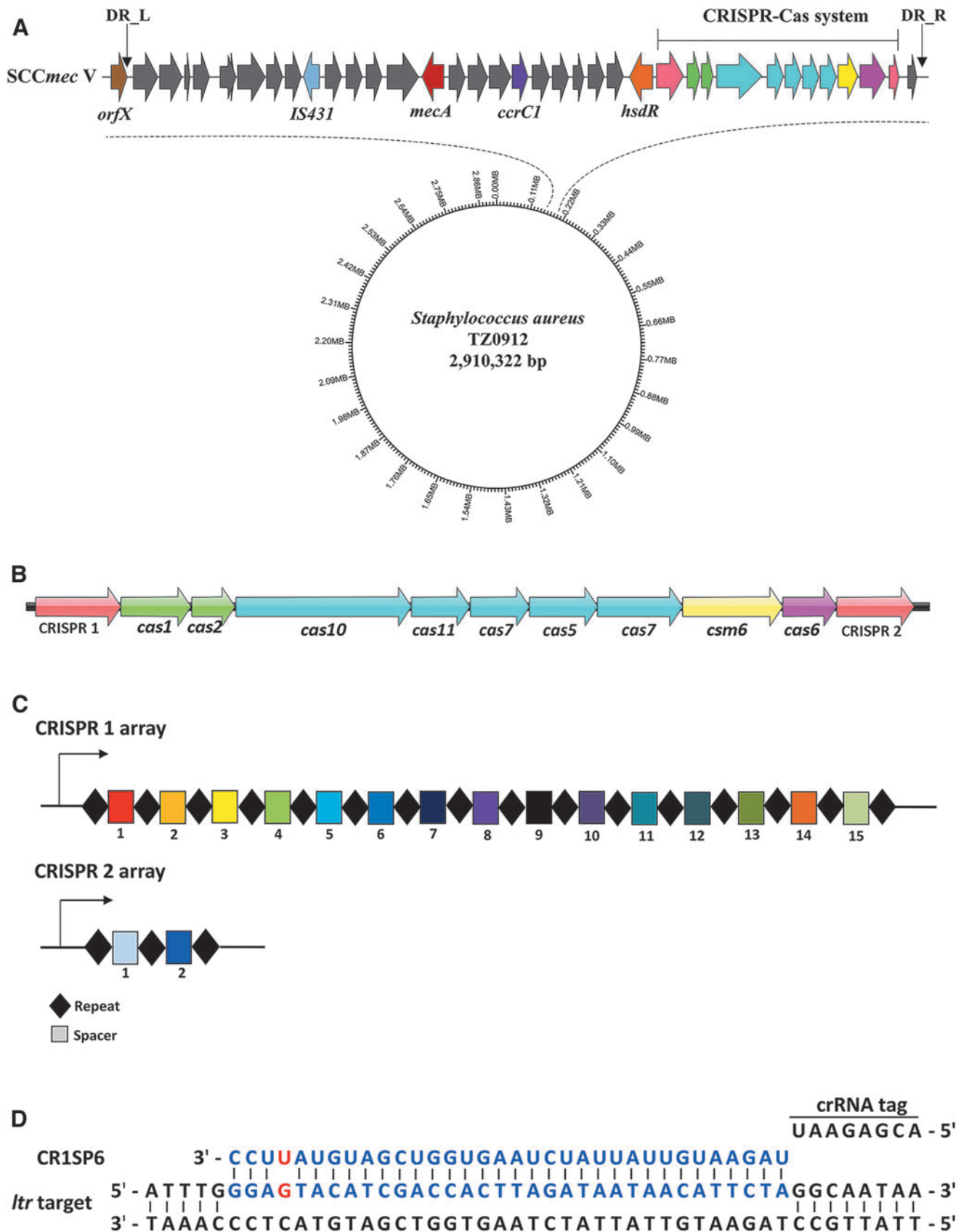
A

DR_L

CRISPR-Cas system

DR_R

SCC*mec* V

orfX   *IS431*   *mecA*   *ccrC1*   *hsdR*

Staphylococcus aureus
TZ0912
2,910,322 bp

B

CRISPR 1   *cas1* *cas2*   *cas10*   *cas11* *cas7* *cas5*   *cas7*   *csm6* *cas6*   CRISPR 2

C

CRISPR 1 array

1 2 3 4 5 6 7 8 9 10 11 12 13 14 15

CRISPR 2 array

1 2

◆ Repeat
▢ Spacer

D

crRNA tag

UAAGAGCA - 5'

CR1SP6   3' - CCUUAUGUAGCUGGUGAAUCUAUUAUUGUAAGAU

ltr target   5' - ATTTGGGAGTACATCGACCACTTAGATAATAACATTCTAGGCAATAA - 3'

            3' - TAAACCCTCATGTAGCTGGTGAATCTATTATTGTAAGATCCGTTATT - 5'

Table 2. Homology Analysis of Spacers in CRISPR Arrays

		Homology analysis	
Spacers	Sequences	No match or y/x[a]	Target for phage/plasmid
CRISPR 1			
Spacer 1	TCTATAAGTTCATTAATTCCGATACCTAGATTATCT	No match	
Spacer 2	TTTTTTCCACCCTTTCAGATCATCTATGATCTTG	No match	
Spacer 3	AATTTTCTAATTCTATAAGTTCATTAATTCCGAT	30/34	*Botulinum prevot*_594 plasmid pCBH
Spacer 4	TATACTATTTACATAATTTTTTATGTGTCTGTCTAC	28/36	*Bacillus* phage G
Spacer 5	TAATAGTGTTGTTCTCTATTAAAAGATACAATCCTGT	No match	
Spacer 6	TAGAATGTTATTATCTAAGTGGTCGATGTATTCC	33/34	*Staphylococcus* phage phiIPLA-RODI, Stab20
Spacer 7	TCTGTAATGTATTCATTTAATGTAATCATAATTTTTC	29/38	*Escherichia coli* Ecol_743 plasmid
Spacer 8	TAGACCATTTACCTCATTATATTTATAGTCTTTATTA	28/37	*Lactococcus* phage P087
Spacer 9	TTTTCTTTAACTGTTTTTACTGCCCATTTAATAGT	32/35	*Staphylococcus* phage phiIPLA-C1C, phiIBB-SEP1
Spacer 10	ATAAACCCGTTCAATTCGTTATCTTTAAATTCTTG	28/35	*Staphylococcus* phage 6ec
Spacer 11	ACAACTTCGTCATCTTTCATCATTTCTCTTACATCA	No match	
Spacer 12	ATATTTCTTCCATGAATAACACCCTCCTTTTTTCTA	28/36	*Lactobacillus plantarum* plasmid pL1277-4
Spacer 13	AAGTTAACGGCATTACCTAATAAAAATATTTTAGG	33/35	*Staphylococcus* phage GRCS, BP39(32), CSA13, SCH1, Pabna, SA4, SLPW, PSa3, SAP-2, phiP68, phi44AHJD Bacteriophage 66
Spacer 14	TCATCTTTCATGTCACTGATTAATTCATTTGTA	31/33	*Staphylococcus* CDC3 plasmid SAP020A
Spacer 15	GGTAATAGTTGCTCAATAGGTAATAAAACGTCGGT	No match	
CRISPR 2			
Spacer1	CTTCTAAGACGCGATATGATTCTAATTGGTCTTC	No match	
Spacer2	GATATACTCCTTTACCATGTATTAATTCTGGACCACT	33/37	*Staphylococcus* phage IME1365_01

[a]The fraction of nucleotide matches between the spacer and the putative protospacer.

and food, respectively. Besides, the 29% of strains (10/35) containing type III-A CRISPR-Cas system belong to CC8 clones.

In order to determine the genetic relatedness of CRISPR-Cas-positive *S. aureus* strains, we generated a maximum-likelihood phylogenetic tree based on single nucleotide polymorphisms in the core genome of the CRISPR-Cas-positive *S. aureus* strain. Thirty-five *S. aureus* genomes were divided into six clades that corresponded well with CC subtypes (Fig. 2). Among the 35 genomes, a total of 34 and 12 unique spacers were identified in the CRISPR 1 and CRISPR 2 array, respectively (Supplementary Table S4). One base mutation in spacer 18 gives rise to the spacer 18 variant. Comparative analysis of the CRISPR spacer arrangement of TZ0912 with the other ST630 *S. aureus* strains showed that 9 of the 15 spacers in CRISPR 1 were conserved among these strains from different geographical locations, while the spacers of CRISPR 2 were completely the same (Fig. 2). Interestingly, the CRISPR 1 locus in these strains has more spacers and shows higher spacer diversity than that of the CRISPR 2 array, suggesting that the spacer adaptation of CRISPR 1 array may be more active. Within ST630, all the strains shared the same *spa* type t4549 and SCC*mec* V (Supplementary Table S3). Our phylogenetic analysis also showed that high genomic identity within ST630 lineage, despite temporal and geographic differences between these strains. For the ST45, the strains containing SCC*mec*

V were relatively closely related and clustered separately from strains with SCC*mec* IV or without SCC*mec* (Fig. 2).

The type III-A CRISPR-Cas system in TZ0912 eliminates plasmids

In order to examine if the CRISPR-Cas system is active in strain TZ0912, we constructed a TZ0912 ΔCRISPR Δ*cas* mutant lacking the entire CRISPR-*cas* region, including the two CRISPR arrays and nine *cas* genes. We also cloned protospacers corresponding to spacer 1, spacer 6, and spacer 14 from the CRISPR 1 array into plasmid pRAB11, giving rise to the plasmids pCR1SP1, pCR1SP6, and pCR1SP14, respectively (Fig. 3A). To assess the ability of CRISPR-Cas to plasmid curing, we monitored target plasmid loss in response to protospacer expression. We observed there was a 90% loss of the pCR1SP1 in the wild-type TZ0912 strain with the induction of ATc for 20 h compared to the empty vector pRAB11, and importantly this difference was abolished in the TZ0912 ΔCRISPR Δ*cas* mutant (Fig. 3B). Interestingly, compared with the pCR1SP1 plasmid, 21% and 41% of the pCR1SP6 and pCR1SP14 plasmid were retained in TZ0912 strain, respectively (Fig. 3B). These results suggested that spacer 6 and spacer 14 provided weaker immunity.

Subsequently, the efficacy of the CRISPR-Cas system was assessed by transforming each of the target plasmids into TZ0912 and TZ0912 ΔCRISPR Δ*cas* and monitoring EOT of the CRISPR-targeted plasmids compared to the
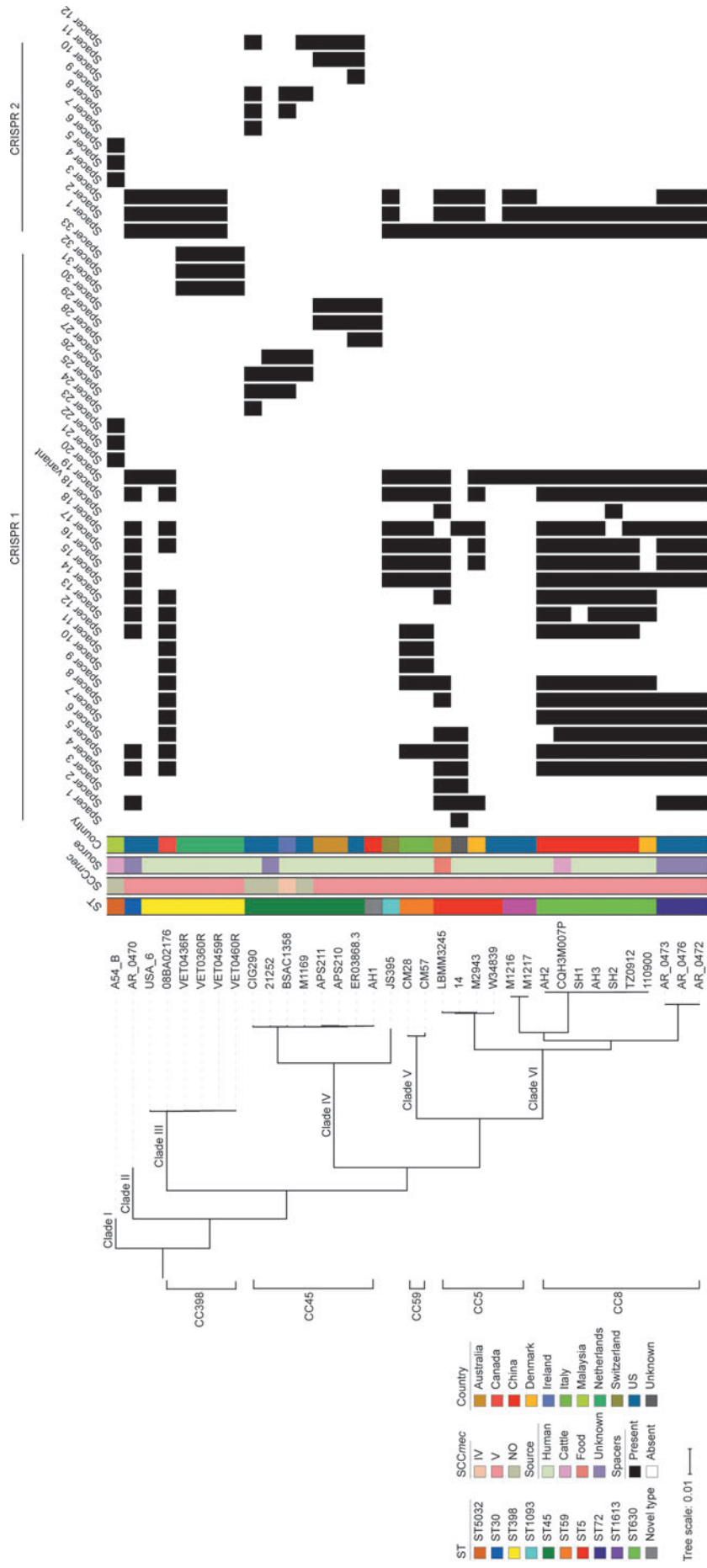
FIG. 2. A maximum likelihood tree of 35 CRISPR-Cas-positive *S. aureus* genomes based on core genome SNP and rooted using the ST5032 A54_B strain. The ST, SCC*mec* type, source, and country of isolation are indicated by *different colors*. The occurrences of spacers were also mapped for each genome. The phylogenetic tree revealed that CRISPR-Cas-positive *S. aureus* are genetically distinct.

empty vector, pRAB11. As shown in Figure 3C, the EOT of pCR1SP1 in TZ0912 was reduced by 60% compared to transformation with the empty pRAB11 plasmid, whereas for pCR1SP6 and pCR1SP14, the EOT was decreased by 40% and 20%, respectively. In the TZ0912 ΔCRISPR Δcas mutant strain, there was no difference in EOT of the empty pRAB11 and of the CRISPR-targeted plasmids (Fig. 3C). Thus, the CRISPR-Cas system in TZ0912 is active, and the crRNAs encoded by the spacers located closest to the 5′ leader sequence of the CRISPR 1 array show highest activity (Fig. 1B), in agreement with previous observations of the type II-A CRISPR system from *Streptococcus pyogenes*.[39] We then analyzed the crRNA expression levels of *S. aureus* TZ0912 by RNA-seq. The crRNA expression showed gradient decline, with the highest abundance for leader-proximal crRNA and lowest abundance for leader-distal crRNAs (Fig. 3D). Interestingly, the crRNA expression profile of the CRISPR 2 array showed a similar pattern with the CRISPR 1 array, and its expression level is higher than that of CRISPR 1 (Supplementary Fig. S2). These results demonstrate that the CRISPR-Cas system in TZ0912 targets plasmids and the efficacy depends on the location of the targeting spacer within the array.

### The CRISPR-Cas system protects TZ0912 from phage attack

It has been shown that the type III-A CRISPR-Cas system in *S. epidermidis* RP62a provides strong immunity against phage mediated killing.[17] To examine if the type III-A CRISPR-Cas system in TZ0912 also protects against phage attack, the wild-type TZ0912 and TZ0912 ΔCRISPR Δcas mutant strains were infected with phage philPLA-RODI at a MOI of 5, and their OD_{600} was measured over time. The phage philPLA-RODI is targeted by the CRISPR 1 spacer 6, except for one nucleotide mismatch (Fig. 1D).

The wild-type TZ0912 exhibited successful immunity against phage infection, while TZ0912 ΔCRISPR Δcas mutant was susceptible to the phage (Fig. 4A). In addition, we infected wild-type TZ0912 and TZ0912 ΔCRISPR Δcas mutant cells in a soft agar overlay with 10-fold dilutions of phage philPLA-RODI. Supplementary Figure S3A showed that philPLA-RODI formed more plaques (most notable at the 10^{-4} dilution) on the lawn of the TZ0912 ΔCRISPR Δcas mutant compared to the wild-type strain (Supplementary Fig. S3A). In order to confirm the functional activity of CRISPR-Cas system further against phage attack between the strains, cultures of TZ0912 and TZ0912 ΔCRISPR Δcas mutant were evenly mixed with the same philPLA-RODI phage concentration (250 PFU) and plated in soft agar overlays. Here, we observed that philPLA-RODI showed an EOP of 32% on strain TZ0912 compared to the TZ0912 ΔCRISPR Δcas mutant (Fig. 4B). Interestingly, philPLA-RODI formed larger plaques on the TZ0912 ΔCRISPR Δcas mutant than those on the wild-type strain (Fig. 4C). Therefore, we compared the expression of the *cas10* and *cas7* genes in liquid culture and solid plate by qRT-PCR analysis. The results showed that the expression level of *cas* genes in liquid culture was twofold higher than that in solid plate ($p < 0.001$; Supplementary Fig. S3B). Collectively, in spite of one mismatch between the CRISPR 1 spacer 6 and the corresponding protospacer sequence located in philPLA-RODI (Fig. 1D), the TZ0912 CRISPR-Cas system is able to protect the cell from phage killing during both the liquid and solid infection.

Discussion

CRISPR-Cas systems provide adaptive immunity for prokaryotes against foreign nucleic acids. However, little is known about the unusually rare CRISPR-Cas systems in clinical isolates of *S. aureus*.[25] In this study, we

FIG. 3. The MRSA TZ0912 CRISPR-Cas system provides immunity against plasmid DNA. **(A)** Diagram of the pRAB11 plasmid and derived plasmids carrying protospacers targeted by CR1SP1, CR1SP6, and CR1SP14, respectively. The protospacers were inserted downstream of the $P_{xy/tet}$ inducible promoter in pRAB11. **(B)** Loss of plasmid assay of the TZ0912 and the TZ0912 ΔCRISPR Δcas mutant carrying the pRAB11 plasmid or the pCR1SP1 (pCR1SP6 or pCR1SP14) plasmid. The strains were grown in TSB with 6 μM anhydrotetracycline (ATc) for 20 h and were plated on TSB with or without chloramphenicol. The assay was carried out in triplicate and repeated four times. The error *bars* represent the standard deviation between each triplicate. **(C)** Transformation efficiencies of the empty plasmid pRAB11 and the CRISPR targeted plasmids in TZ0912 and the TZ0912 ΔCRISPR Δcas mutant with 6 μM ATc. The transformation efficiencies of the CRISPR targeted plasmids were normalized to those of the vector, pRAB11. Results are the means ± standard deviation (*SD*) of at least three independent experiments. ***$p < 0.001$ (*t*-test). **(D)** Visualization of CRISPR 1 array transcription profiles of TZ0912. RNA-seq reads were mapped to the *S. aureus* TZ0912 genome to determine the relative abundance of individual crRNA by Integrative Genomics Viewer software. The vertical *dotted line* marks the position of the spacers in CRISPR 1 array.
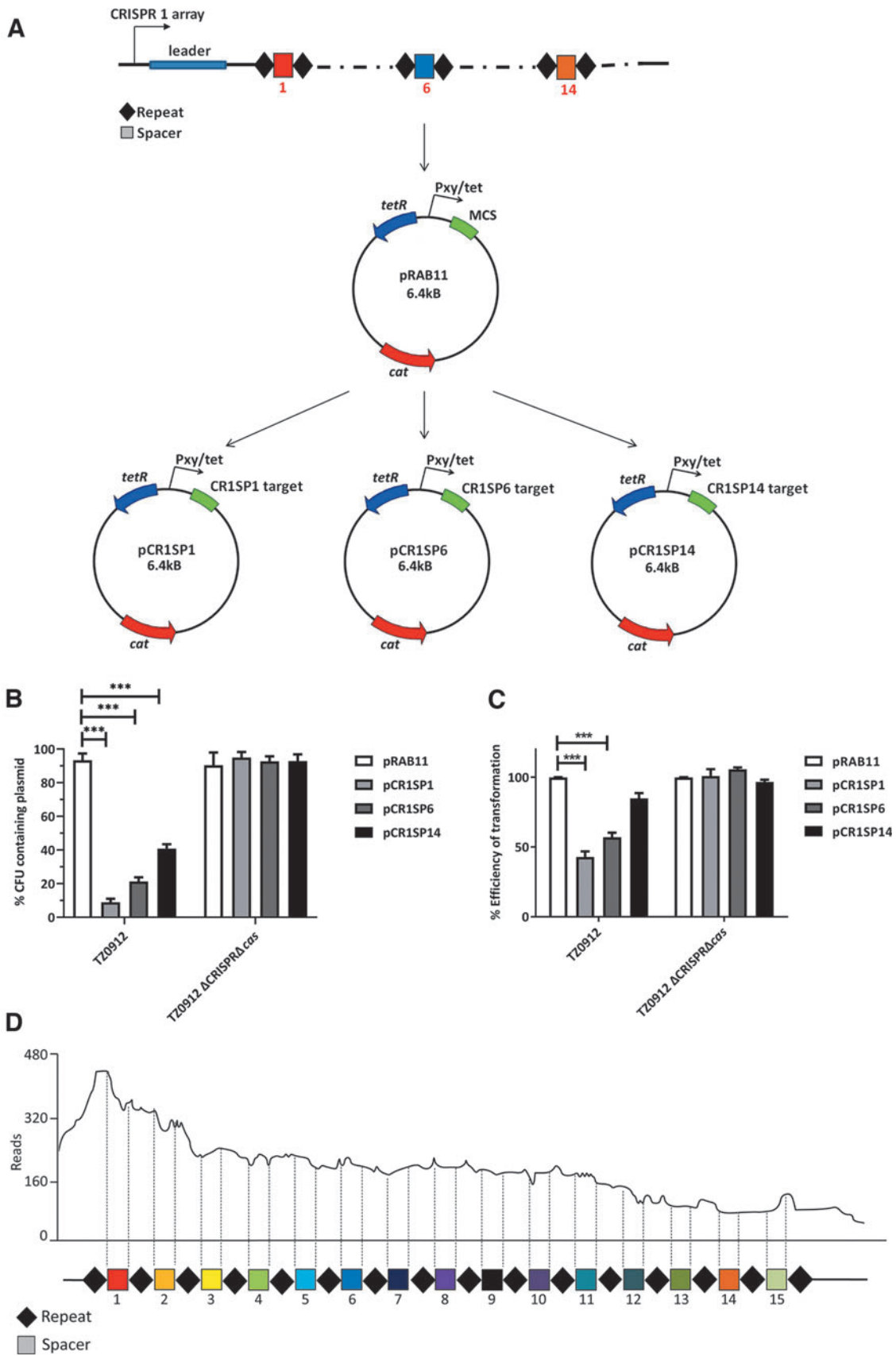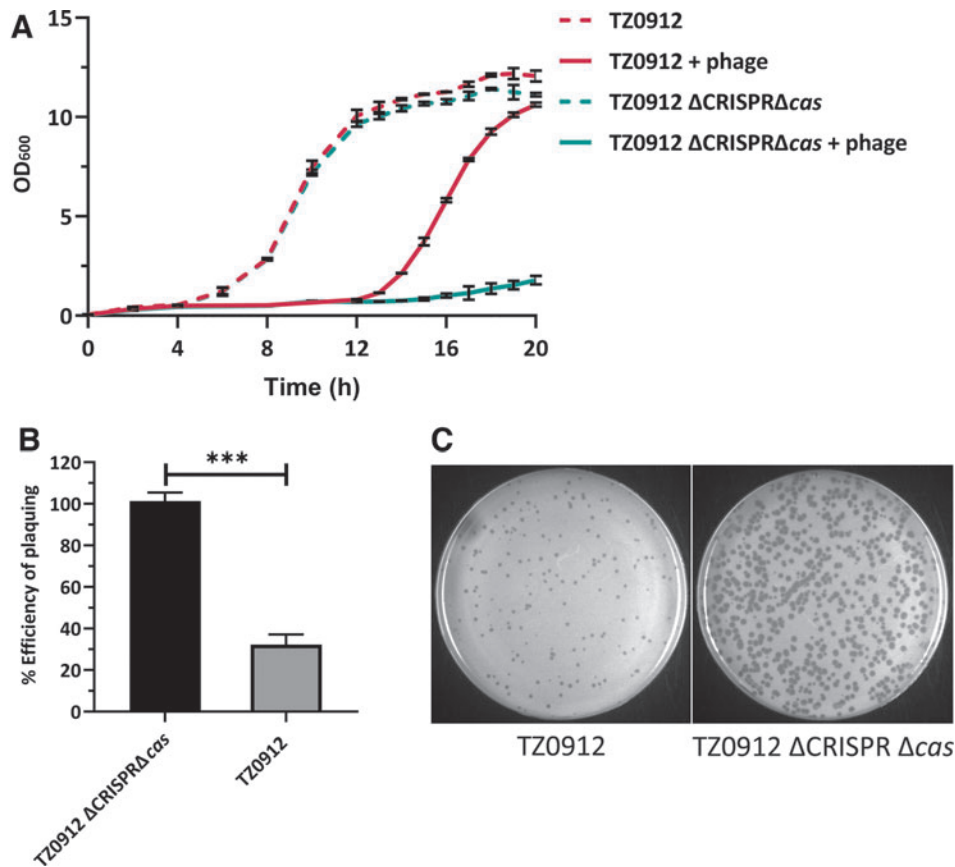
FIG. 4. The MRSA TZ0912 CRISPR-Cas system provides immunity against phage phiIPLA-RODI. **(A)** Growth curves of liquid cultures of TZ0912 and TZ0912 ΔCRISPR Δcas infected with phage phiIPLA-RODI at a multiplicity of infection of 5 alongside uninfected controls. Results from three biological replicates are shown, and error *bars* indicate the corresponding *SD*. **(B)** Efficiency of plaquing (relative to the number of plaques formed in lawns of TZ0912 ΔCRISPR Δcas mutant) of phage phiIPLA-RODI on lawns of TZ0912 and the TZ0912 ΔCRISPR Δcas mutant. Results are the means ± *SD* of at least three independent experiments. ***$p < 0.001$ (*t*-test). **(C)** The plaque size of phiIPLA-RODI on lawns of TZ0912 and TZ0912 ΔCRISPR Δcas mutant. Overnight cultures were mixed with 250 PFU phiIPLA-RODI and plated in a soft agar overlay and incubated overnight.

investigated the MRSA strain TZ0912, which was isolated from a patient with a skin infection in China. We found that TZ0912 harbors a type III-A CRISPR-Cas system. Our investigation of CRISPR-Cas-positive *S. aureus* genomes and phylogenetic tree analysis revealed that the CRISPR-Cas-positive strains were genetically distinct and mainly belong to CC8 clones. We showed that the endogenous type III-A CRISPR-Cas system in TZ0912 is active and can protect the bacterium from plasmid transformation and phage infection. Interestingly, we found that the CRISPR-Cas system was more active against phage when the cells were grown in liquid culture compared to when they were grown on a solid surface (Fig. 4 and Supplementary Fig. S3B). These results correlated with a recent study showing higher CRISPR-

Cas activity of the type I-F CRISPR-Cas system in *Pseudomonas aeruginosa* in liquid cultures and CRISPR-Cas repression in biofilm growth,[40] suggesting that this phenomenon could be universal among CRISPR-Cas-positive bacteria. We also demonstrated that the immune capacity of spacers was closely related to the distance between the spacer and the CRISPR leader sequence at the 5′ end of the CRISPR array. RNA-seq analysis further confirmed that the leader end protospacers were more abundantly expressed than the more distal protospacers.

CRISPR-Cas systems are underrepresented in *S. aureus* strains. Cao *et al.* detected only 0.94% of clinical *S. aureus* strains from China harbor complete type III-A CRISPR-Cas systems.[25] From our analysis of the published *S. aureus* genomes in the NCBI database, we

identified 35 *S. aureus* genomes bearing type III-A CRISPR-Cas. Of these 35 strains, 10 belong to CC8 clone, indicating that the CRISPR-cas system is prevalent in the CC8 clone. Although the 08BA02176 and TZ0912 with other ST630 strains possess similar CRISPR arrays, they were not co-localized on the same cluster due to their different ST types, suggesting that the CRISPR-Cas system may have undergone a horizontal transfer between different ST types. Consistent with previously reported strains of ST type and *spa* type,[25] clinical MRSA TZ0912 also belongs to the ST630/t4549 clonal complex. Notably, ST630 has been reported to be a common human-associated MRSA clone, causing skin and soft-tissue infection in China.[41] However, one ST630/t4549 clone recovered from Denmark was also found to harbor type III-A CRISPR-Cas system, which implied that the CRISPR-Cas-positive ST630/t4549 clone could spread globally.

CRISPR spacer sequences determine CRISPR-mediated immunity and are mainly derived from phages or plasmids that have previously attacked or parasitized bacteria.[42] In the MRSA TZ0912 strain, 41.18% (7/17) of spacers show homology with phage genomes (Table 2), suggesting that the TZ0912 strain primarily uses its CRISPR-Cas system for fighting off phage. Since CRISPR 1 was diverse with more spacers than CRISPR 2, this study focused on CRISPR 1 to investigate the expression difference of spacers located at the leader-proximal and leader-distal regions. Interestingly, the strains 08BA02176, CM28, and CM57 each have two unique spacers (spacer 10 and 11) in the middle of the array compared to ST630 strains, which suggests that ectopic adaptation may happen in CRISPR arrays of these strains. It has also been shown that the mutation of leader anchoring sequence can cause adaptation of new spacers in the middle of an array.[39] However, the alignment of leader sequences between the strains 08BA02176, CM28, and CM57 and the ST630 strains showed that no mutations occur in these leader sequences (data not shown). In addition, none of the spacers in the CRISPR arrays showed a perfect match to protospacers in plasmids or phages, suggesting that the targeted protospacer sequences in the genetic elements have acquired ''escape'' mutations that allow them to avoid or reduce CRISPR interference.[43]

While the crRNA maturation is critical for the immunity of CRISPR-Cas system against foreign nucleic acids, we have found that the location of spacer can also determine the ability of immunity, with the first spacer providing 60% plasmid immunity and spacer 14 providing only 20% immunity in this study, in agreement with previous findings.[39] The crRNA expression in CRISPR 1 array showed gradient decrease, with the highest abundance for leader end crRNA and lowest abundance for distal crRNA. These results are consistent with previous reports showing that the crRNAs derived from spacers close to leader end are more abundantly expressed and provide stronger immunity than crRNAs produced from downstream spacers.[39,44]

A programmable CRISPR-Cas system from *S. epidermidis* RP62a transformed into *S. aureus* provides strong immunity against plasmids and phages.[36] Compared to the strong CRISPR-based resistance levels to plasmid conjugation observed in *S. epidermidis*,[2] the CRISPR-Cas interference levels of *S. aureus* TZ0912 against targeted plasmids and phage philPLA-RODI in a soft agar overlay is relatively low. One possible explanation for this is that one of the prophages carried on the TZ0912 chromosome could express an anti-CRISPR gene. Further, we observed that the staphylococcal system appears to be more active against phage compared to plasmid. This could potentially be due to a hitherto uncharacterized anti-CRISPR element on the plasmid analogous to what was recently found for a type II-A system[45] or that entry of plasmid and phage is differentially recognized. In addition, a recent study showed that Rcs stress response can inversely regulate the cell-surface receptors versus CRISPR-Cas immunity to discriminate plasmids invasion and phages infection.[46]

Unlike type I and type II CRISPR-Cas interference, which phages can avoid relatively easily by acquiring mutations abolishing sequence recognition of the crRNA seed or the protospacer adjacent motif, type III-A CRISPR-Cas systems work robustly, even with some degree of mismatch between crRNA and the protospacer sequence.[47] To this end, we find that the TZ0912 type III-A CRISPR-Cas system provides robust immunity against killing by the phage philPLA-RODI in both liquid culture and solid medium, even though it has a 1 bp mismatch with spacer 6 (Fig. 1D). However, in a classical soft agar overlay assay, the CRISPR-Cas-dependent immunity against phage philPLA-RODI infection was less pronounced, indicating that CRISPR-Cas may be inhibited by a surface attachment-based mechanism. Such a mechanism was recently discovered in *P. aeruginosa* PA14, where the type I-F CRISPR-Cas system is inhibited by the alginate regulator AmrZ exclusively when the cells are attached to a surface.[40]

Recently, phage therapy has been intensively studied and was proposed to treat *S. aureus* infections.[48] However, if CRISPR-Cas is indeed emergent among MRSA strains, this may prove a challenge for future phage therapy efforts against MRSA infections. This study demonstrates that the type III-A CRISPR-Cas system in MRSA can effectively defend from phage infection via spacers homologous to the phage genome. Therefore, our work

provides a model system to evaluate the impact of the type III CRISPR-Cas system against phage therapies in clinical MRSA isolates.

Conclusion

In summary, we found that the type III-A CRISPR-Cas system was prevalent in *S. aureus* CC8 clones. With the characterization of the CRISPR-Cas system in MRSA TZ0912, we determined that the system provided immunity against both plasmids and phage infection. Importantly, the CRISPR-Cas system in TZ0912 was more active against phage when the cells grown in liquid culture than that in solid agar. We further demonstrated that the efficiency of immunity was dependent on the location of spacers in type III-A CRISPR-Cas system.

Acknowledgments

Author Disclosure Statement

The authors declare no competing interests.

Funding Information

Supplementary Material

Supplementary Sequence Data
Supplementary Table S1
Supplementary Table S2
Supplementary Table S3
Supplementary Table S4
Supplementary Figure S1
Supplementary Figure S2
Supplementary Figure S3

References

1. Barrangou R, Fremaux C, Deveau H, et al. CRISPR provides acquired resistance against viruses in prokaryotes. *Science* 2007;315:1709–1712. DOI: 10.1126/science.1138140.

2. Marraffini LA, Sontheimer EJ. CRISPR interference limits horizontal gene transfer in *Staphylococci* by targeting DNA. *Science* 2008;322:1843–1845. DOI: 10.1126/science.1165771.

3. Burstein D, Sun CL, Brown CT, et al. Major bacterial lineages are essentially devoid of CRISPR-Cas viral defence systems. *Nat Commun* 2016;7:10613. DOI: 10.1038/ncomms10613.

4. Makarova KS, Wolf YI, Iranzo J, et al. Evolutionary classification of CRISPR-Cas systems: a burst of class 2 and derived variants. *Nat Rev Microbiol* 2020;18:67–83. DOI: 10.1038/s41579-019-0299-x.

5. Mohanraju P, Makarova KS, Zetsche B, et al. Diverse evolutionary roots and mechanistic variations of the CRISPR-Cas systems. *Science* 2016;353:aad5147. DOI: 10.1126/science.aad5147.

6. Amitai G, Sorek R. CRISPR-Cas adaptation: insights into the mechanism of action. *Nat Rev Microbiol* 2016;14:67–76. DOI: 10.1038/nrmicro.2015.14.

7. Cady KC, White AS, Hammond JH, et al. Prevalence, conservation and functional analysis of *Yersinia* and *Escherichia* CRISPR regions in clinical *Pseudomonas aeruginosa* isolates. *Microbiology* 2011;157:430–437. DOI: 10.1099/mic.0.045732-0.

8. Nuñez JK, Lee ASY, Engelman A, et al. Integrase-mediated spacer acquisition during CRISPR–Cas adaptive immunity. *Nature* 2015;519:193–198. DOI: 10.1038/nature14237.

9. Yosef I, Goren MG, Qimron U. Proteins and DNA elements essential for the CRISPR adaptation process in *Escherichia coli*. *Nucleic Acids Res* 2012;40:5569–5576. DOI: 10.1093/nar/gks216.

10. Hatoum-Aslan A, Maniv I, Marraffini LA. Mature clustered, regularly interspaced, short palindromic repeats RNA (crRNA) length is measured by a ruler mechanism anchored at the precursor processing site. *Proc Natl Acad Sci U S A* 2011;108:21218–21222. DOI: 10.1073/pnas.1112832108.

11. Hatoum-Aslan A, Maniv I, Samai P, et al. Genetic characterization of antiplasmid immunity through a type III-A CRISPR-Cas system. *J Bacteriol* 2014;196:310–317. DOI: 10.1128/jb.01130-13.

12. Chou-Zheng L, Hatoum-Aslan A. A type III-A CRISPR-Cas system employs degradosome nucleases to ensure robust immunity. *Elife* 2019;8. DOI: 10.7554/eLife.45393.

13. Kazlauskiene M, Tamulaitis G, Kostiuk G, et al. Spatiotemporal control of type III-A CRISPR-Cas immunity: coupling DNA degradation with the target RNA recognition. *Mol Cell* 2016;62:295–306. DOI: 10.1016/j.molcel.2016.03.024.

14. Samai P, Pyenson N, Jiang W, et al. Co-transcriptional DNA and RNA cleavage during type III CRISPR-Cas immunity. *Cell* 2015;161:1164–1174. DOI: 10.1016/j.cell.2015.04.027.

15. Kazlauskiene M, Kostiuk G, Venclovas Č, et al. A cyclic oligonucleotide signaling pathway in type III CRISPR-Cas systems. *Science* 2017;357:605–609. DOI: 10.1126/science.aao0100.

16. Niewoehner O, Garcia-Doval C, Rostol JT, et al. Type III CRISPR-Cas systems produce cyclic oligoadenylate second messengers. *Nature* 2017;548:543–548. DOI: 10.1038/nature23467.

17. Jiang W, Samai P, Marraffini Luciano A. Degradation of phage transcripts by CRISPR-associated RNases enables type III CRISPR-Cas immunity. *Cell* 2016;164:710–721. DOI: 10.1016/j.cell.2015.12.053.

18. Rostøl JT, Marraffini LA. Non-specific degradation of transcripts promotes plasmid clearance during type III-A CRISPR–Cas immunity. *Nat Microbiol* 2019;4:656–662. DOI: 10.1038/s41564-018-0353-x.

19. Bondy-Denomy J, Pawluk A, Maxwell KL, et al. Bacteriophage genes that inactivate the CRISPR/Cas bacterial immune system. *Nature* 2013;493:429–432. DOI: 10.1038/nature11723.

20. Patterson AG, Jackson SA, Taylor C, et al. Quorum sensing controls adaptive immunity through the regulation of multiple CRISPR-Cas systems. *Mol Cell* 2016;64:1102–1108. DOI: 10.1016/j.molcel.2016.11.012.

21. Høyland-Kroghsbo NM, Paczkowski J, Mukherjee S, et al. Quorum sensing controls the *Pseudomonas aeruginosa* CRISPR-Cas adaptive immune system. *Proc Natl Acad Sci U S A* 2017;114:131–135. DOI: 10.1073/pnas.1617415113.

22. Patterson AG, Chang JT, Taylor C, et al. Regulation of the type I-F CRISPR-Cas system by CRP-cAMP and GalM controls spacer acquisition and interference. *Nucleic Acids Res* 2015;43:6038–6048. DOI: 10.1093/nar/gkv517.

23. Høyland-Kroghsbo NM, Muñoz KA, Bassler BL. Temperature, by controlling growth rate, regulates CRISPR-Cas activity in *Pseudomonas aeruginosa*. *mBio* 2018;9:e02184–02118. DOI: 10.1128/mBio.02184-18.

24. Westra Edze R, van Houte S, Oyesiku-Blakemore S, et al. Parasite exposure drives selective evolution of constitutive versus inducible defense. *Curr Biol* 2015;25:1043–1049. DOI: 10.1016/j.cub.2015.01.065.

25. Cao L, Gao C-H, Zhu J, et al. Identification and functional study of type III-A CRISPR-Cas systems in clinical isolates of *Staphylococcus aureus*. *Int J Med Microbiol* 2016;306:686–696. DOI: 10.1016/j.ijmm.2016.08.005.

26. Chambers HF. Methicillin resistance in *Staphylococci*: molecular and biochemical basis and clinical implications. *Clin Microbiol Rev* 1997;10:781–791. DOI: 10.1128/CMR.10.4.781-791.1997.

27. Holt DC, Holden MTG, Tong SYC, et al. A very early-branching *Staphylococcus aureus* lineage lacking the carotenoid pigment staphyloxanthin. *Genome Biol Evol* 2011;3:881–895. DOI: 10.1093/gbe/evr078.

28. Golding GR, Bryden L, Levett PN, et al. Livestock-associated methicillin-resistant *Staphylococcus aureus* sequence type 398 in humans, Canada. *Emerg Infect Dis* 2010;16:587–594. DOI: 10.3201/eid1604.091435.

29. Kinnevey PM, Shore AC, Brennan GI, et al. Emergence of sequence type 779 methicillin-resistant *Staphylococcus aureus* harboring a novel pseudo staphylococcal cassette chromosome *mec* (SCC*mec*)-SCC-SCC-CRISPR composite element in Irish hospitals. *Antimicrob Agents Chemother* 2013;57:524–531. DOI: 10.1128/aac.01689-12.

30. Larsen J, Andersen PS, Winstel V, et al. *Staphylococcus aureus* CC395 harbours a novel composite staphylococcal cassette chromosome *mec* element. *J Antimicrob Chemother* 2017;72:1002–1005. DOI: 10.1093/jac/dkw544.

31. Li Q, Xie X, Yin K, et al. Characterization of CRISPR-Cas system in clinical *Staphylococcus epidermidis* strains revealed its potential association with bacterial infection sites. *Microbiol Res* 2016;193:103–110. DOI: 10.1016/j.micres.2016.09.003.

32. Couvin D, Bernheim A, Toffano-Nioche C, et al. CRISPRCasFinder, an update of CRISRFinder, includes a portable version, enhanced performance and integrates search for Cas proteins. *Nucleic Acids Res* 2018;46:W246–W251. DOI: 10.1093/nar/gky425.

33. Biswas A, Gagnon JN, Brouns SJJ, et al. CRISPRTarget: bioinformatic prediction and analysis of crRNA targets CRISPRTarget. *RNA Biol* 2013;10:817–827. DOI: 10.4161/rna.24046.

34. Treangen TJ, Ondov BD, Koren S, et al. The Harvest suite for rapid core-genome: alignment and visualization of thousands of intraspecific microbial genomes. *Genome Biol* 2014;15:524. DOI: 10.1186/s13059-014-0524-x.

35. Helle L, Kull M, Mayer S, et al. Vectors for improved Tet repressor-dependent gradual gene induction or silencing in *Staphylococcus aureus*. *Microbiology* 2011;157:3314–3323. DOI: 10.1099/mic.0.052548-0.

36. Goldberg GW, Jiang W, Bikard D, et al. Conditional tolerance of temperate phages via transcription-dependent CRISPR-Cas targeting. *Nature* 2014;514:633–637. DOI: 10.1038/nature13637.

37. Monk IR, Shah IM, Xu M, et al. Transforming the untransformable: application of direct transformation to manipulate genetically *Staphylococcus aureus* and *Staphylococcus epidermidis*. *mBio* 2012;3. DOI: 10.1128/mBio.00277-11.

38. Thorvaldsdottir H, Robinson J, Mesirov JP. Integrative Genomics Viewer (IGV): high-performance genomics data visualization and exploration. *Brief Bioinform* 2012;14:178–192. DOI: 10.1093/bib/bbs017.

39. McGinn J, Marraffini Luciano A. CRISPR-Cas systems optimize their immune response by specifying the site of spacer integration. *Mol Cell* 2016;64:616–623. DOI: 10.1016/j.molcel.2016.08.038.

40. Borges AL, Castro B, Govindarajan S, et al. Bacterial alginate regulators and phage homologs repress CRISPR–Cas immunity. *Nat Microbiol* 2020;5:679–687. DOI: 10.1038/s41564-020-0691-3.

41. Chen W, He C, Yang H, et al. Prevalence and molecular characterization of methicillin-resistant *Staphylococcus aureus* with mupirocin, fusidic acid and/or retapamulin resistance. *BMC Microbiol* 2020;20:183. DOI: 10.1186/s12866-020-01862-z.

42. Marraffini LA. CRISPR-Cas immunity in prokaryotes. *Nature* 2015;526:55–61. DOI: 10.1038/nature15386.

43. Künne T, Zhu Y, da Silva F, et al. Role of nucleotide identity in effective CRISPR target escape mutations. *Nucleic Acids Res* 2018;46:10395–10404. DOI: 10.1093/nar/gky687.

44. Richter H, Zoephel J, Schermuly J, et al. Characterization of CRISPR RNA processing in *Clostridium thermocellum* and *Methanococcus maripaludis*. *Nucleic Acids Res* 2012;40:9887–9896. DOI: 10.1093/nar/gks737.

45. Mahendra C, Christie KA, Osuna BA, et al. Broad-spectrum anti-CRISPR proteins facilitate horizontal gene transfer. *Nat Microbiol* 2020;5:620–629. DOI: 10.1038/s41564-020-0692-2.

46. Smith LM, Jackson SA, Malone LM, et al. The Rcs stress response inversely controls surface and CRISPR-Cas adaptive immunity to discriminate plasmids and phages. *Nat Microbiol* 2021;6:162–172. DOI: 10.1038/s41564-020-00822-7.

47. Pyenson NC, Gayvert K, Varble A, et al. Broad targeting specificity during bacterial type III CRISPR-Cas immunity constrains viral escape. *Cell Host Microbe* 2017;22:343–353.e3. DOI: 10.1016/j.chom.2017.07.016.

48. Petrovic Fabijan A, Lin RCY, Ho J, et al. Safety of bacteriophage therapy in severe *Staphylococcus aureus* infection. *Nat Microbiol* 2020;5:465–472. DOI: 10.1038/s41564-019-0634-z.